COLEÇÃO

DESAFIOS DAS ENGENHARIAS:

ENGENHARIA DE COMPUTAÇÃO 2

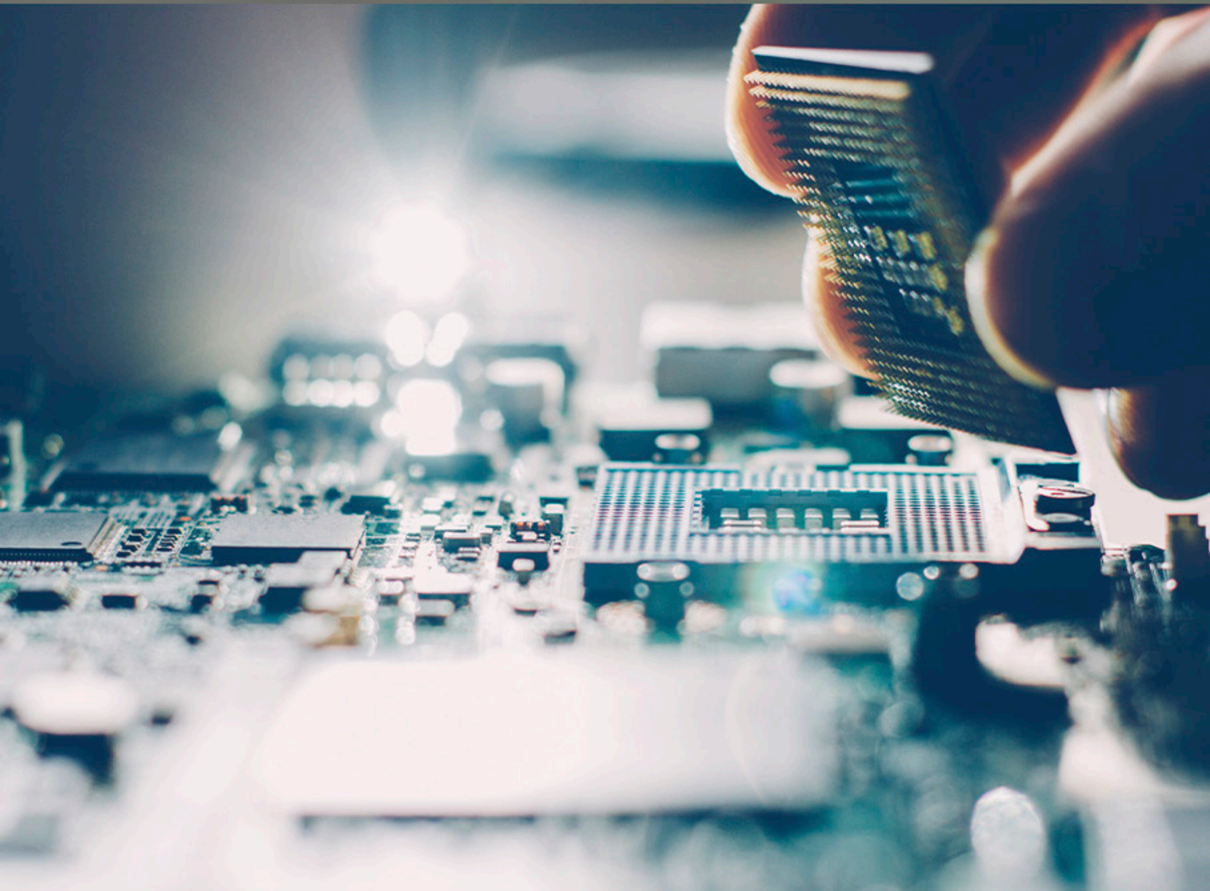

ERNANE ROSA MARTINS
(ORGANIZADOR)

Atena Editora
Ano 2021

COLEÇÃO

DESAFIOS DAS ENGENHARIAS:

ENGENHARIA DE COMPUTAÇÃO 2

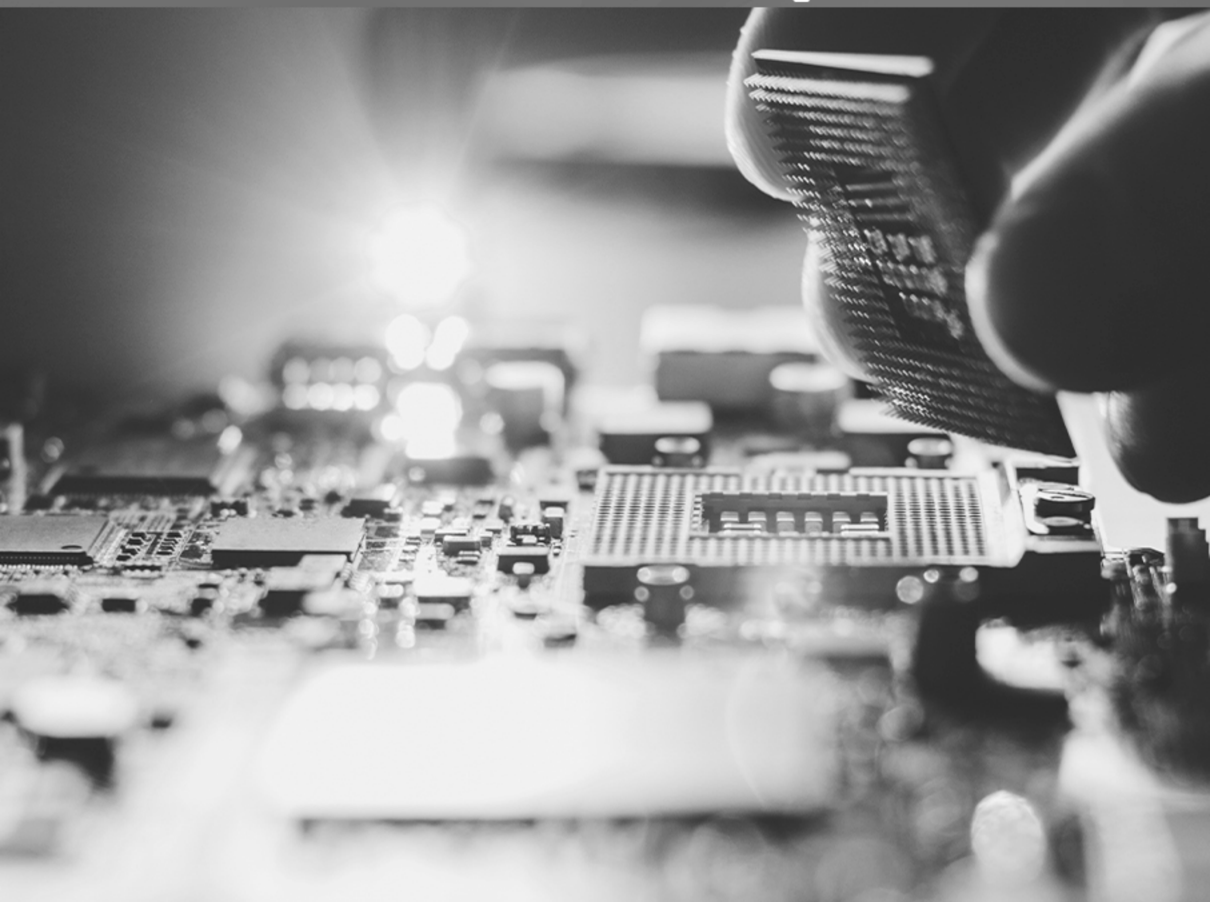

ERNANE ROSA MARTINS
(ORGANIZADOR)

Atena Editora
Ano 2021

Editora chefe
Profª Drª Antonella Carvalho de Oliveira
Assistentes editoriais
Natalia Oliveira
Flávia Roberta Barão
Bibliotecária
Janaina Ramos
Projeto gráfico
Natália Sandrini de Azevedo
Camila Alves de Cremo
Luiza Alves Batista
Maria Alice Pinheiro
Imagens da capa
iStock
Edição de arte
Luiza Alves Batista
Revisão
Os autores

Atena Editora
Ano 2021

Ciências Exatas e da Terra e Engenharias

Atena Editora
Ano 2021

Atena Editora
Ano 2021

Ciências Exatas e da Terra e Engenharias

Ciências Exatas e da Terra e Engenharias

Atena Editora
Ano 2021

Ciências Exatas e da Terra e Engenharias

Coleção desafios das engenharias: engenharia de computação 2

Diagramação: Maria Alice Pinheiro
Correção: Giovanna Sandrini de Azevedo
Indexação: Gabriel Motomu Teshima
Revisão: Os autores
Organizador: Ernane Rosa Martins

Dados Internacionais de Catalogação na Publicação (CIP)

C691 Coleção desafios das engenharias: engenharia de computação 2 / Organizador Ernane Rosa Martins. – Ponta Grossa - PR: Atena, 2021.

Formato: PDF
Requisitos de sistema: Adobe Acrobat Reader
Modo de acesso: World Wide Web
Inclui bibliografia
ISBN 978-65-5983-384-9
DOI: https://doi.org/10.22533/at.ed.849211808

1. Engenharia da computação. I. Martins, Ernane Rosa (Organizador). II. Título.

CDD 621.39

Elaborado por Bibliotecária Janaina Ramos – CRB-8/9166

Atena Editora
Ponta Grossa – Paraná – Brasil
Telefone: +55 (42) 3323-5493
www.atenaeditora.com.br
contato@atenaeditora.com.br

Atena Editora
Ano 2021

DECLARAÇÃO DOS AUTORES

Os autores desta obra: 1. Atestam não possuir qualquer interesse comercial que constitua um conflito de interesses em relação ao artigo científico publicado; 2. Declaram que participaram ativamente da construção dos respectivos manuscritos, preferencialmente na: a) Concepção do estudo, e/ou aquisição de dados, e/ou análise e interpretação de dados; b) Elaboração do artigo ou revisão com vistas a tornar o material intelectualmente relevante; c) Aprovação final do manuscrito para submissão.; 3. Certificam que os artigos científicos publicados estão completamente isentos de dados e/ou resultados fraudulentos; 4. Confirmam a citação e a referência correta de todos os dados e de interpretações de dados de outras pesquisas; 5. Reconhecem terem informado todas as fontes de financiamento recebidas para a consecução da pesquisa; 6. Autorizam a edição da obra, que incluem os registros de ficha catalográfica, ISBN, DOI e demais indexadores, projeto visual e criação de capa, diagramação de miolo, assim como lançamento e divulgação da mesma conforme critérios da Atena Editora.

Atena Editora
Ano 2021

DECLARAÇÃO DA EDITORA

A Atena Editora declara, para os devidos fins de direito, que: 1. A presente publicação constitui apenas transferência temporária dos direitos autorais, direito sobre a publicação, inclusive não constitui responsabilidade solidária na criação dos manuscritos publicados, nos termos previstos na Lei sobre direitos autorais (Lei 9610/98), no art. 184 do Código penal e no art. 927 do Código Civil; 2. Autoriza e incentiva os autores a assinarem contratos com repositórios institucionais, com fins exclusivos de divulgação da obra, desde que com o devido reconhecimento de autoria e edição e sem qualquer finalidade comercial; 3. Todos os e-book são *open access, desta forma* não os comercializa em seu site, sites parceiros, plataformas de *e-commerce,* ou qualquer outro meio virtual ou físico, portanto, está isenta de repasses de direitos autorais aos autores; 4. Todos os membros do conselho editorial são doutores e vinculados a instituições de ensino superior públicas, conforme recomendação da CAPES para obtenção do Qualis livro; 5. Não cede, comercializa ou autoriza a utilização dos nomes e e-mails dos autores, bem como nenhum outro dado dos mesmos, para qualquer finalidade que não o escopo da divulgação desta obra.

APRESENTAÇÃO

A Engenharia de Computação é a área que estuda as técnicas, métodos e ferramentas matemáticas, físicas e computacionais para o desenvolvimento de circuitos, dispositivos e sistemas. Esta área tem a matemática e a computação como seus principais pilares. O foco está no desenvolvimento de soluções que envolvam tanto aspectos relacionados ao software, quanto à elétrica/eletrônica. Os profissionais desta área são capazes de atuar principalmente na integração entre software e hardware, tais como: automação industrial e residencial, sistemas embarcados, sistemas paralelos e distribuídos, arquitetura de computadores, robótica, comunicação de dados e processamento digital de sinais.

Dentro deste contexto, esta obra aborda diversos aspectos tecnológicos computacionais, tais como: implementação e modificações numéricas a serem feitas no algorítmo de Anderson (2010) para simular o escoamento sobre uma asa finita submetida a ângulos de ataque próximos ao estol; modelo distribuído para analisar a influência da formação e do adensamento de geada sobre o desempenho de evaporadores do tipo tubo-aletado, comumente usados em refrigeradores frost-free; um algoritmo de Redes Neurais Convolucionais(CNN) que identifica se a pessoa está ou não utilizando a máscara; potencialidades do M-Learning e Virtual Reality no curso técnico em Agropecuária; avaliação da qualidade da energia elétrica em um sistema de geração de energia fotovoltaica; uma abordagem para a segmentação de imagens cerebrais, utilizando o método baseado em algoritmos genéticos pelo método de múltiplos limiares; estudo numérico de uma âncora torpedo sem aletas cravada em solo isotrópico puramente coesivo, utilizando um modelo axissimétrico não-linear em elementos finitos; estudo acerca da análise numérica de placas retangulares por meio do método das diferenças finitas, obtendo soluções aproximadas para o campo de deslocamentos transversais bem como os correspondentes momentos fletores, para problemas envolvendo uma série de condições de contorno, utilizando-se o software Matlab® para simulação; desenvolvimento e aplicação da Realidade Virtual (RV) como Tecnologia de Informação e Comunicação (TIC) para auxiliar no processo de ensino-aprendizado de disciplinas do Ensino Médio; avaliação dos resultados obtidos em campanhas de medição de qualidade da energia elétrica (QEE) na rede básica em 500 kV; examinar o comportamento mecânico-estático de uma longarina compósita projetada para uma aeronave esportiva leve através de investigações numéricas, empreendidas em software (ANSYS Release 19.2) comercial de elementos finitos; construção de um sistema para monitoramento de ativos públicos; a relação da Sociedade 5.0 envolvida no contexto da Indústria 4.0 e a Transformação Digital; algoritmos de seleção e de classificação de atributos, identificando as vinte principais características que contribuem para o desempenho alto ou baixo dos estudantes; a Mask R-CNN, utilizada para a segmentação de produtos automotivos (parabrisas, faróis, lanternas, parachoques e retrovisores) em uma empresa do ramo de reposição automotiva; o nível de usabilidade do aplicativo protótipo para dispositivo móvel na área da saúde voltado ao auxílio do monitoramento móvel no uso de medicamentos em seres humanos.

Sendo assim, está obra é significativa por ser composta por uma gama de trabalhos pertinentes, que permitem aos seus leitores, analisar e discutir diversos assuntos importantes desta área. Por fim, desejamos aos autores, nossos mais sinceros agradecimentos pelas significativas contribuições, e aos nossos leitores, desejamos uma proveitosa leitura, repleta de boas reflexões.

Ernane Rosa Martins

SUMÁRIO

CAPÍTULO 8

MODELLING AND ANALYSIS OF AEROBOAT JAHU

Data de aceite: 02/08/2021

João B. de Aguiar
Professor, Engenharia Aeroespacial,
Universidade Federal do ABC
Santo André

Júlio C.S. Sousa
Engineer, Universidade Federal do ABC
Santo André

José M. de Aguiar
Professor, Departamento de Ensino, FATEC-SP
Praça Col. Fernando Prestes, São Paulo

ABSTRACT: Jahu was the name of the first plane to cross the Atlantic with a Brazilian crew. The saga of such a voyage is described in the literature, being well documented, as the fact attracted large media coverage. It took place in the 1920 decade. The hydroplane itself is not well known, however, mostly due to modifications introduced for the journey. Particulars of Jahu like its high weight, the use of a pair of in-line external engines with propellers in opposite directions and large lateral floats, led people to call it the flying boat. Making an ocean cross with this airplane required a sequence of stops to solve problems; some caused by sabotage others by design and lots of courage. In this research, starting from the drawings of the plane, a model of the structure was constructed. Flight coupled to flow equations were solved to infer the lift and drag forces in the structure of the aeroboat. Finite element equations were then employed to determine response of the structure. Results showed the plane as being very sound. Procedure used may help construct for similar problems.

KEYWORDS: Model, Flow Problem, Motion, Stress Problem, Reliability.

RESUMO: O Jahu foi o primeiro avião a cruzar o Atlântico com uma tripulação brasileira. A saga dessa viagem é descrita na literatura, documentadamente, uma vez que o fato atraiu uma grande cobertura dos meios de comunicação. Ocorreu nos anos 1920. O aeroplano, contudo, não é bem conhecido, principalmente por conta das modificações introduzidas para e durante a jornada. Particularidades da aeronave, como o elevado peso, uso de um par de motores alinhados, com pás de hélice girando em sentido contrário, e a presença de grandes flutuadores, levou as pessoas a chama-lo de barco voador. No cruzar do oceano, uma sequência de paradas, para resolver problemas, alguns causados por sabotagem, outros por erros de projeto, ocorreram. Nesta pesquisa, a partir dos desenhos da aeronave, um modelo da estrutura é construído. Equações de voo acopladas às de aerodinâmica são apresentadas a fim de estabelecer as resultantes de sustentação e arrasto na estrutura do "aerobote". Da mesma forma as equações para as tensões na estrutura são formuladas. Discretização por elemento finito é utilizada para determinar a resposta da estrutura. Diversos resultados são apresentados e discutidos. Conclui-se ser bastante rígido o avião. O modelo desenvolvido pode ajudar na construção de uma réplica do hidroavião.

PALAVRAS - CHAVE: Modelo, Problema de Fluxo, Movimento, Problema das Tensões.

1 I INTRODUCTION

A hydroplane Savoia-Marchetti S.55, version C, constructed in Italy, reequipped with two 550 hp engines and enhanced floaters was used by João Ribeiro de Barros to cross the Atlantic South in 1927. Prior records of velocity and authonomy made the hidro a preferred choice of Barros and its three crew members. Jahu, as it was named was the first to cross in direct flight the ocean from Cape Verde, a Portuguese archipelago, to Fernando de Noronha, an island in northeast Brazil, non-stop.

The first crossing of the south Atlantic in 1922 by Gago Coutinho and Sacadura Cabral inspired João Ribeiro, natural of Jau, new graphy for the name of the city of Jahu, interior of São Paulo state, to organize a raid. In fact, Gago Coutinho and Sacadura Cabral also helped João Ribeiro to plan the trip. However distant, the idea became possible after another pioneer of aviation, *conde Casagrande* with a Savoia-Marchetti S-55C named Alcyone, gave up a travel from Italy to Argentina, when only one fifth of the trip was completed. With the desistance, the Alcyone was returned to the SIAI, the manufacturer of the plane.

João Ribeiro, after understanding be the S-55 the best plane to the endeavor, tried to buy a brand new one from SIAI, the maker of S-55, with no success. A selling offer for Alcyone was presented, instead. The deal was set after some requested modifications to the S-55 were agreed upon. Jahu, Fig. 1, was delivered in October 1926. Voyage started when it took off from Genova, Italy towards Gibraltar. Five hours later, however, the engines of Jahu started to present problems, and an emergency stop in the bay of Valencia, Spain, extended to Alicante, took place. Jahu´s crew ended up jailed, as landing was not authorized nor intended. Solved the case with diplomatic help, the plane flew to Gibraltar, where better conditions permitted repairing the engines, victims of sabotage. Direct distance to Gibraltar is about 496 km.

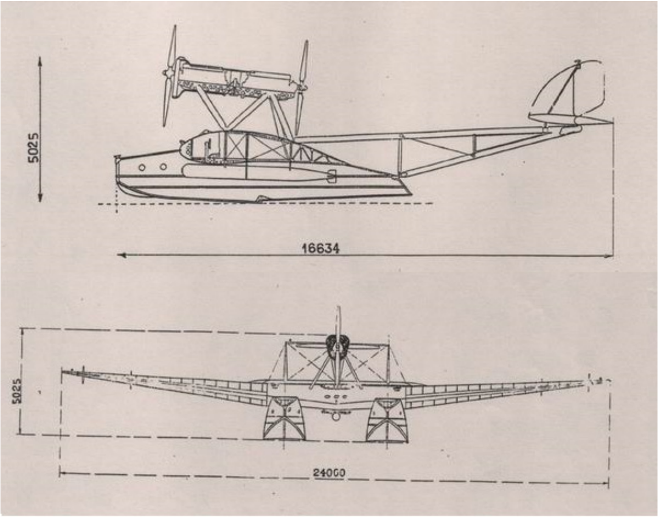

Fig. 1. Lateral and frontal view drawings of Jahu.

In the next stretch Canary Islands, in the Atlantic Ocean, distant some 1 324 km from Gibraltar, were reached, again at the cost of great efforts from the crew. Failures in the fuel system of the engines required manual feeding. This time the problem was in the pumping system. Solved, next stop was in *Praia*, city in *Cape Verde Islands*, distant 1 646 km of *Gran Canária*. A larger stop was taken then, as major changes had to be implemented to prepare the airplane for the most difficult part of the raid.

The stop in *Praia* was plagued by problems. Several mechanical modifications had to be tried and tested. Also a change in command: a lieutenant from São Paulo, Newton Braga had to be sent to *Praia* after the pilot refused to fly the plane again. After months on the stop, malaria fevers convalescences, general disbelief from public, João Ribeiro received an encouraging letter from his mother that made him proceed with the voyage.

Repaired, the hydro took off in April 1927. During 12 hours, it flew at an average velocity of 190 km/h and 250 m high to reach Fernando de Noronha, in a non-stop journey. Distance was record for an airplane on those days. It was a moment of great jubilee in Brazil. Trip followed then along the Brazilian coast: cities of Natal, 375 km, Recife, 254 km, Salvador circa of 672 km from Recife and Rio de Janeiro, 1209 km away, were reached. After another large stop in Rio in an ambient of fiesta, last part of raid took place, with arrival in São Paulo in August of 1927. After that, Jahu wouldn´t fly again.

2 | MODEL

Determination of the stresses in the hydroplane, at any instant, requires knowledge of motion and aerodynamic equations as they set up the loading. To this end, the body of the plane was first drawn from construction blueprints. Next, a model, with the corresponding equations, was considered having in mind unveil a solution procedure. Although several flight scenarios are possible, they all obey the same set of equations of conservation and some constitutive models. Even though a particular scenario, the level flight, is of interest here, a general look at the problem is important.

Hence, solution of the dynamic problem coupled to the pressure-velocity field is discussed first. Stresses in the airplane structure, which depend on the obtained results, are then computed and factors of safety in the elastic range computed.

2.1 Conservation Equations

Airflow around an airplane gives rise to contact stresses that actuate on its skin. The resultants of this interaction depend on plane configuration and relative velocity $\mathrm{V}_r = \mathrm{V}_b - \mathrm{V}_a$, where V_b refers to airboat velocity and V_a to the air velocity. Standard model procedure considers a control volume V_c, with border surface S_c used to include and move with the plane. Values of airflow variables, which include the velocity v_a, the pressure p_a and temperature T_a of air, for every plane velocity, which obey the conservation equations, are sought. First equation, air mass conservation, $M_a = 0$ says that [3]:

$$\frac{\partial}{\partial t}\int_{V_c}\rho_a dV + \int_{S_c}\rho_a \mathbf{v}_a \cdot \mathbf{n} dS = 0 \tag{1}$$

where density of air is denoted as ρ_a. Control surface contains an inner part that contacts the plane S_c^b and another external, the outer border S_c^a, where free flow conditions apply, being $S_c = S_c^b \cup S_c^a$. Control volume partition follows the same procedure.

Next pair of equations represents the conservation of the linear momentum L_a with $\mathbf{l}_a = \rho_a v_a$, and conservation of the angular momentum H_a with $\mathbf{h}_a = \rho_a \mathbf{r}_a \times \mathbf{v}_a$, of the air surrounding the plane:

$$\frac{\partial}{\partial t}\int_{V_c}\mathbf{l}_a dV + \int_{S_c}\mathbf{l}_a \mathbf{v}_a \cdot \mathbf{n} dS = \int_{V_c}\mathbf{b}_a dV + \int_{S_c}\{-p_a\mathbf{n} + \tau_a \mathbf{t}\} dS \tag{2}$$

$$\frac{\partial}{\partial t}\int_{V_c}\mathbf{h}_a dV + \int_{S_c}\mathbf{h}_a \mathbf{v}_a \cdot \mathbf{n} dS = \int_{V_c}\mathbf{r}_a \times \mathbf{b}_a dV + \int_{S_c} r_{\mathbf{a}} \times \{-p_a\mathbf{n} + \tau_a \mathbf{t}\} dS \tag{3}$$

In these equations, bod y forces denoted as $\mathbf{b}_a$ include inertia forces. Surface tractions comprise normal p_a and tangential τ_a components. Symbol x is used to indicate the cross product between position vector r_a, with respect to an inertial reference system $< x,y;z >$, and velocity vector v_a in the angular momentum expression. Scalar product is shown with a dot.

First integral in right hand side of Eq. (2) represents the resultant body force, whereas the second corresponds to the resultant surface force. In both integrals, resultants over the plane, inner border, are computed from the resultants in the outer border of control volume. Integration of the pressure and tangential stresses lead to the lift $\boldsymbol{L}$ and drag $\mathbf{D}$ forces. Likewise, integrals in the right hand side of Eq. (3) indicate the corresponding moments, with respect to the reference system. These resultant forces and moments are required inputs for the structural problem. Energy conservation, that would couple the expressions, is not considered here.

2.2 Flight Equations

Motion of the airplane depends on the interaction of applied forces, propulsion included, with aerodynamics forces. Given the geometry of the plane, body and applied forces - instant weight $\mathbb{W}$ and propellers thrust $\mathbb{E}$, established by settings of the engine group and control surfaces – solution of the dynamic problem will define the kinematics of the plane. Newton's second law constitutes the basic equilibrium equation to solve. It establishes that the rate of change of the linear momentum $\int_{V_c^b} \mathbf{l}_b \, dV$ on the plane equals the summation of external forces applied to it $\mathbf{I}_b = \mathbf{p}_b \mathbf{v}_b$. Hence if b, with the subscript identifying the aeroboat, then [4]:

$$\frac{d}{dt} \int_{V_c^b} \mathbf{l}_b \, dV = \mathbf{F}_a + \mathbf{W} + \mathbf{E} \tag{4}$$

being the air interaction resultant:

$$\mathbf{F}_a = \int_{V_c^b} \mathbf{b}_a \, dV + \int_{S_c^b} \{-p_a \mathbf{n} + \tau_a \mathbf{t}\} dS \tag{5}$$

This sum includes added mass plus lift $\mathbb{L}$ and drag $\mathbb{D}$ resultants. The set of components of the differential equation Eq. (4) - $M_b a_b = \sum F$ - depends on time. However, loading on right hand side also depends on time, through the velocity components. Solution renders the linear acceleration of the plane. Rigid solid approximation will relate local accelerations to the center of mass acceleration, making it easier the solution. Successive integration of accelerations will establish the velocity field and trajectory. An iterative substitution procedure may be employed, taking an initial estimate of the aerodynamic resultant, Eq. (5).

In the same form, the rate of change of the angular momentum $\int_{V_c^b} \mathbf{h}_b dV$, where $\mathbf{h}_b = r_\mathbf{b} \times \mathbf{v}_b$, equals the summation of the moments of the external efforts:

$$\frac{\partial}{\partial t} \int_{V_c^b} \mathbf{h}_b dV = \sum_b \mathbf{M} \tag{6}$$

which comprises the moment resultant from air flux:

$$\mathbf{M}_a = \int_{V_c^p} \mathbf{r}_b \times \mathbf{b}_a \, dV + \int_{S_c^a} \mathbf{r}_b \times \{-p_a \mathbf{n} + \tau_a \mathbf{t}\} dS \tag{7}$$

plus the moment contributions from applied forces pair < $\mathbb{W}$, $\mathbb{E}$ >. This new set of equations - $I_b \boldsymbol{\alpha}_\mathbf{b} = \sum_b M$ - will define the angular accelerations and their kinematic relatives.

2.3 Velocity and Pressure Field

At the instant tagging the flight scenario, solution of the fluid-structure interaction problem, and afterwards stress problem, may be attained by the principle of virtual work, PVW. One form of this principle sets the rate of internal work to the rate of external work exchange [5]:

$$\int_{V_c} \delta\dot{\boldsymbol{\varepsilon}}_a{}^T \boldsymbol{\sigma}_a \, dV = \int_{V_c} \delta\mathbf{v}_a{}^T \mathbf{b}_a \, dV + \int_{S_c} \delta\mathbf{v}_a{}^T \{-p_a \mathbf{n} + \tau_a \mathbf{t}\} \, dS \quad (8)$$

where $\boldsymbol{\sigma}_a$ represents the Cauchy stress tensor, ε_a is the strain rate tensor:

$$\dot{\boldsymbol{\varepsilon}}_a = \frac{1}{2}\{\nabla\mathbf{v}_a + \nabla\mathbf{v}_a{}^{\mathbf{T}}\} \quad (9)$$

being ∇ the gradient operator. Symbol *δ* indicates virtual quantities and matrix notation is supposed.

Writing the air velocity field in terms of its Cartesian components, $\mathbf{v}_a{}^T = \{\dot{u}_a, \dot{v}_a, \dot{w}_a\}$, where the set $< u_a, v_a, w_a >$ identifies the components of the displacement field, renders the strain rate tensor ε_a in terms of v_a field. A linear operator $\mathcal{L}_a$ relates both quantities as:

$$\dot{\boldsymbol{\varepsilon}}_a = \mathcal{L}_a \mathbf{v}_a \quad (10)$$

Additionally, if inertia forces are separated from the set of body forces, $b_a = b_a^i + b_a^o$, virtual work expression, Eq. (8), changes to the form:

$$\int_{V_c} \delta\mathbf{v}_a{}^T \boldsymbol{L}_a{}^{\boldsymbol{T}} \boldsymbol{\sigma}_a dV - \int_{V_c} \delta\mathbf{v}_a{}^T \mathbf{b}_a^o dV - \int_{S_c} \delta\mathbf{v}_a{}^T (-p_a \mathbf{n} + \tau_a \mathbf{t}) dS = \int_{V_c} \delta\mathbf{v}_a{}^T \rho_a \mathbf{a}_a dV \quad (11)$$

being the accelerations dependent of time and position:

$$\mathbf{a}_a = \mathbf{v}_{a,t} + \nabla\mathbf{v}_a \, \mathbf{v}_a \quad (12)$$

The specific constitutive equation relating stresses to strain rates may now be included [5]. For incompressible fluids, with moderate velocities involved, temperature coupling may be disregarded and Navier-Stokes relationship assumed. This equation relates deviatoric components of stress to strain rates:

$$\boldsymbol{\sigma}'_a = \boldsymbol{C}'_{\boldsymbol{a}} \, \dot{\boldsymbol{\varepsilon}}_a ; \quad \boldsymbol{\sigma}'_a = \boldsymbol{\sigma}_a + p_a \mathbf{I} \quad (13)$$

where the deviatoric part C'_a of the constitutive tensor C_a depends on viscosity. Pressure is the negative trace of stress tensor $p_a = -tr\,\boldsymbol{\sigma}_a$ but it cannot be determined in the above equation, requiring hence, an additional constitutive expression. Upon introduction of the above relation, Eq. (9) into the expression of the PVW it results that:

$$\int_{V_c} \delta\mathbf{v}_a{}^T \rho_a \mathbf{a}_a dV = \int_{V_c} \delta\mathbf{v}_a{}^T \mathcal{L}_\alpha{}^T \mathcal{C}'_\alpha \mathcal{L}_\alpha \mathbf{v}_a dV - \int_{V_c} \delta\mathbf{v}_a{}^T \mathcal{L}_\alpha{}^T p_a \mathbf{I} dV - \int_{V_c} \delta\mathbf{v}_a{}^T \mathbf{b}_a^o dV - \int_{S_c} \delta\mathbf{v}_a{}^{\mathbf{T}} \{-p_a \mathbf{n} + \tau_a \mathbf{t}\} dS \qquad (14)$$

being I the identity tensor. This equation may be solved numerically using spatial discretization by finite elements with time marching algorithms. In the process, internal variables are written in terms of nodal quantities by means of interpolation functions, for velocity and pressure. Therefore, if the relations

$$\begin{aligned} \mathbf{v}_a &= \mathbf{N}^v \hat{\mathbf{v}}_a \\ p_a &= \mathbf{N}^p \hat{\mathbf{p}}_a \end{aligned} \qquad (15)$$

are introduced into Eq. (10), with nodal quantities identified with the hat, it turns out that:

$$\mathbf{M}_a \frac{\partial}{\partial t} \hat{\mathbf{v}}_a + \{\mathbf{K}_l^v + \mathbf{K}_{nl}^v\} \hat{\mathbf{v}}_a + \mathbf{K}^p \hat{\mathbf{p}}_a = \mathbf{R}_V + \mathbf{R}_\mathbf{s} \qquad (16)$$

where mass, velocity-stiffness – linear and non-linear, and pressure-stiffness matrices are, respectively:

$$\mathbf{M}_a = \int_{V_c} \mathbf{N}^{v^T} \rho_a \mathbf{N}^v dV \qquad (17)$$

$$\mathbf{K}_l^v = \int_{V_c} \mathbf{B}^{v^T} \mathcal{C}'_\alpha \mathbf{B}^v dV \qquad (18)$$

$$\mathbf{K}_{nl}^v = \int_{V_c} \rho_a \mathbf{N}^{v^T} \{\nabla(\mathbf{N}^v \hat{\mathbf{v}}_a)^T\} \mathbf{N}^v dV \qquad (19)$$

$$\mathbf{K}^p = \int_{V_c} \mathbf{B}^{v^T} \mathbf{I} \mathbf{N}^p dV \qquad (20)$$

being $\mathbf{B}^v$ the strain-velocity interpolation matrix. Resultant vectors:

$$\mathbf{R}_v = \int_{V_c} \mathbf{N}^{v^T} \mathbf{b}_a dV \qquad (21)$$

$$\mathbf{R}_S = \int_{S_c} \mathbf{N}^{v^T} (-p_a \mathbf{I} + \boldsymbol{\tau}_a) dS \qquad (22)$$

represent the overall resultants of the body and surface forces, in this order.

The discretized finite element system, Eq. (16), depends on the nodal velocities and pressures. Therefore, an additional equation has to be prescribed in order to complete the system to be solved in the flow problem. The remaining equation, conservation of mass, Eq. (1), may be used, in discretized form. Using the pressure as a virtual Lagrange multiplier, under stead state conditions, leads to the additional condition:

$$\int_{V_c} \delta p_a^{\ T} (\nabla^T \mathbf{v}_a) dV = 0 \tag{23}$$

because $div\,\mathbf{v}_a = \nabla^T \mathbf{v}_a = 0$. However as:

$$\begin{aligned} p_a &= \mathbf{N}^p \hat{p}_a \\ \nabla^T \mathbf{v}_a &= \mathbf{B}^v \hat{\mathbf{v}}_a \end{aligned} \tag{24}$$

so that the inclusion of these results into the restriction equation, Eq. (23), leads to:

$$\mathbf{K}^{p^T} \hat{\mathbf{v}}_a = 0 \tag{25}$$

which allows solution of the pressure-velocity field.

2.4 Iterative Substitution Procedure

Loading to the airplane could be approached in different manners. An iterative substitution procedure is an alternative. In such a case, initial estimate of linear and angular velocity of the airplane, set the applied loads, may be obtained from the above formulation using the pair of flight equations, Eqs, (4) and (6), with an initial guess for the pair $< L_0, D_0 >$.

With the determined accelerations, and then velocity vectors, the aerodynamic problem may be solved using Eq. (16) with the condition Eq. (25) imposed, leading to a first fluid velocity-pressure distribution. Air may be supposed still. New integrated resultants for lift and drag are obtained $< L_1, D_1 >$. Back substitution of the results brings a new plane velocity. At level flight, the convergence is fast.

2.5 Airplane Stresses

Once found the velocity field around the plane, loading at the tagged position is determined, stresses and deformations may be found. Application of the PVW to the plane in such a case leads to [6]:

$$\int_{V_b} \delta\mathbf{v}_b^{\ T} \boldsymbol{\sigma}_b dV = \int_{V_b} \delta\mathbf{v}_b^{\ T} \mathbf{b}_b dV + \int_{S_p} \delta\mathbf{v}_b^{\ T} \{-p_a \mathbf{n} + \tau_a \mathbf{t}\} dS + \delta\mathbf{v}_b^{\ T} \mathbf{E} \tag{26}$$

This equation depends on the velocity field $\mathbf{v}_b$, on the contact stresses on aeroboat´s surface, a function of the air velocity, body forces and thrust. Discretizing the space occupied by the airplane by volume elements - with required air and structure meshes coinciding at plane surface - by means of interpolation functions N^v give:

$$\mathbf{v}_b = N^v \hat{\mathbf{v}}_b \tag{27}$$

Taking the stress-strain relationship in the elastic range for the different materials of the boat as $\mathbf{C}_b$ leave:

$$\boldsymbol{\sigma}_b = C_p \, \boldsymbol{\varepsilon}_b ; \quad \boldsymbol{\varepsilon}_b = \mathbf{B}^d \, \hat{\mathbf{d}}_b \tag{28}$$

with $\hat{\mathbf{d}}_p$ referring to nodal displacements. Hence equilibrium in the sense of Eq. (26) requires that:

$$\mathbf{M}_b \frac{\partial^2}{\partial t^2}\hat{\mathbf{d}}_b + \mathbf{K}_b \hat{\mathbf{d}}_b = \mathbf{R}_b \quad (29)$$

Here $\mathbf{R}_b$ stands for the sum of the external forces and $\mathbf{M}_b$ for the consistent mass – derived from the separation of the body forces into inertia and all others effects, $\mathbf{b}_b = \mathbf{b}_b^i + \mathbf{b}_b^o$ of the aeroboat. When accelerations are small, the quasi-static solution of the equation will render the displacement field, and the interpolation and constitutive equations, the stresses. Undamped dynamics effects may also be determined from Eq. (29) [7].

3 I RESULTS

3.1 Geometry

Jahu was designed with four main structural systems: a pair of wings, a pair of floating boats, as it was a hydroplane, and a truss structure to sustain the engines and the control surfaces located at the back of the plane. Very compact and heavy units set side by side with opening bays, like in the truss system, placed the center of mass of the hydroplane quite low, conferring stability. A part this fact, the plane required the constant use of horizontal stabilizer surfaces to acquire equilibrium in level flight conditions, making this system vital. Overall characteristics of the plane are included in Table 1.

Wings were designed with 3D lifting surfaces of variable section, cambered, with constant angle of attack, and laterally disposed about a frontal plane, perpendicular to the main longitudinal symmetry plane, Figures 2 and 3. Arching and thinning was provided along the span of the wings in order to create multiple curvature of the outer shell surface. Solid and open forms were used for the aerodynamic profile elements and stiffeners in the wing.

Maximum Wing Span	24 m
Maximum Length	16.75 m
Height	5.0 m
Wing Area	93.0 m^2
Aileron Surface Area	3.60 m^2
Horizontal Stabilizer Area	11.0 m^2
Vertical Stabilizer Area	4.40 m^2

Table 1. Main characteristics of Jahu.

Transverse reinforcing beam elements were the central elements of the wing arrangement. In it, a primary rib structure supported the series of aerodynamic elements responsible for flexural resistance of the wing. The plate structure of aerodynamic elements contained movable components. Tertiary structure included shell elements of skin that covers the wing. Arrangement was completed with movable – aileron and flap – as well as tail surfaces.

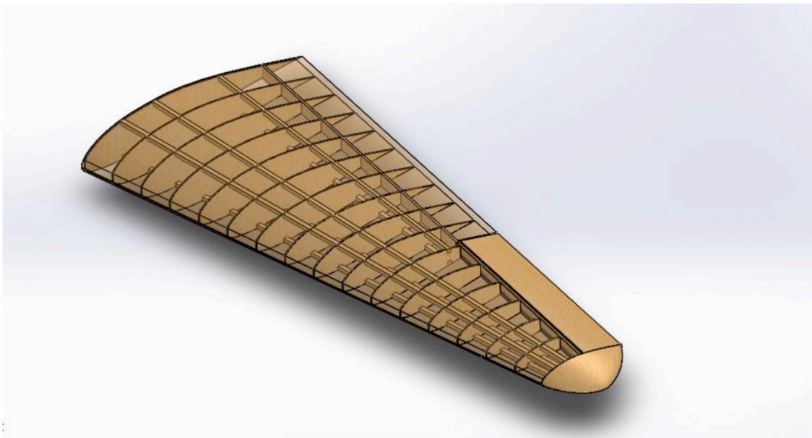

Fig. 2. External semi-wing structure drawing.

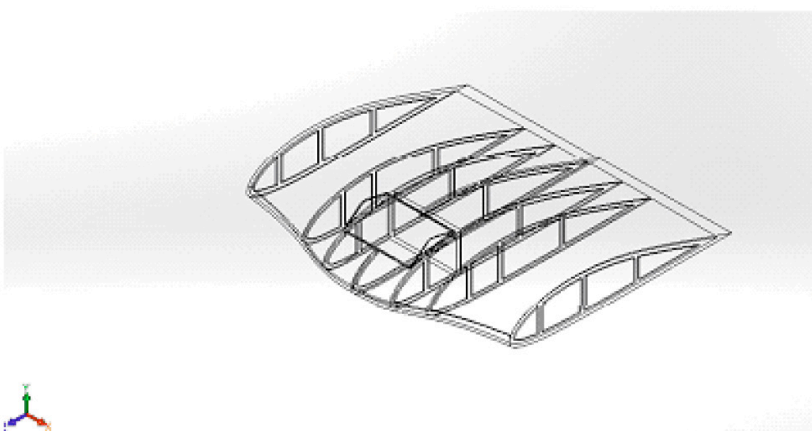

Fig. 3. Central part of the wing system.

The floating boats, *scafos* as the Italians called them, were arranged with a system of transverse rings, supported by longitudinal stiffeners, covered by a quite rigid skin system, Fig. 4. Forms were chosen with two curvatures adjusted to diminish the drag with water and air. They were disposed symmetrically about the longitudinal plane, fixed to the wings and placed in a lower level. Each boat comported two crew members, one of them a pilot, as the plane required two pilots.

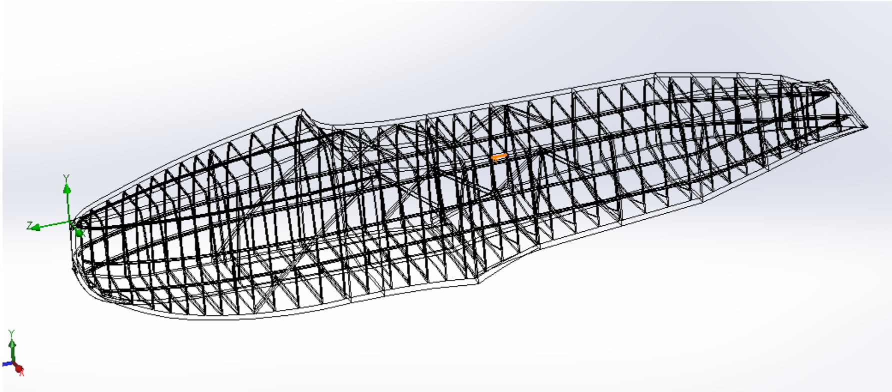

Fig. 4. Structural arrangement of the boats.

The longitudinal fuselage system comprised two complementary parts, one responsible for supporting the engines, set on top of the longitudinal plan, in symmetric form, and the other responsible for holding the control surfaces, located at the back of the plane, Fig. 5. Both structures were made of 1D structural elements, beams and bars. They were integrated with the wings and floating boats systems. The upper support system for the pair of engines comprised truss units with two bays. Crossing cables were included to avoid sway motion. Engines were centrally disposed with shaft axes placed inclined.

The control surfaces were disposed in horizontal and vertical planes in the tail of the plane. In the vertical plane, a small fin was used in conjunction with a pair of identical larger lateral units, for flow stability. Structural arrangement followed quite closely that one of the wings, using however much thinner elements for the rudder. Rotational motion was about a central post in the vertical direction. Part of the horizontal surface was capable of rotation with respect to a horizontal axis operated by means of linkages.

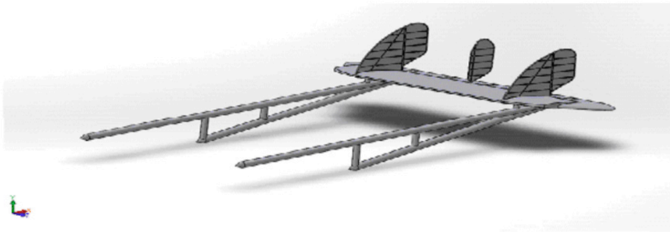

Fig. 5. Tail structure with supporting truss.

3.2 Flow Pattern

Velocity and height reached during trip trajectory by Jahu were quite low, reason why flow was approximately non-turbulent all over its skin. A part the region close to the propellers of the engines, not taken into account in the simulation, laminar conditions were found in most of the flow field around of the body of the hydro, Fig. 6. Flow processor of program SolidWorks [8] was employed to the task. Level flight conditions were taken, under standard atmospheric conditions.

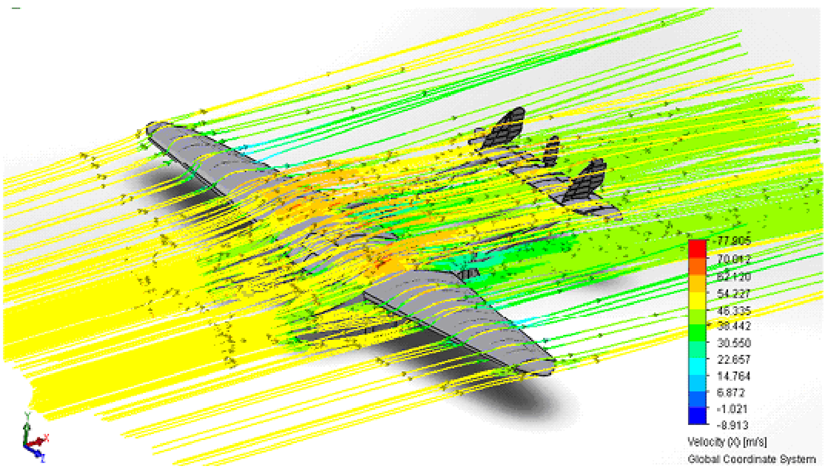

Fig. 6. Velocity field around the Jahu model.

Pressure distribution in the flow problem appears in Fig. 7, for the same conditions. From the plot, it is seen that borders of attack of the outer wings have higher pressures: peak values appear under these wings. Moreover, most of the drag in the plane comes out of the large boats; also, crew space.

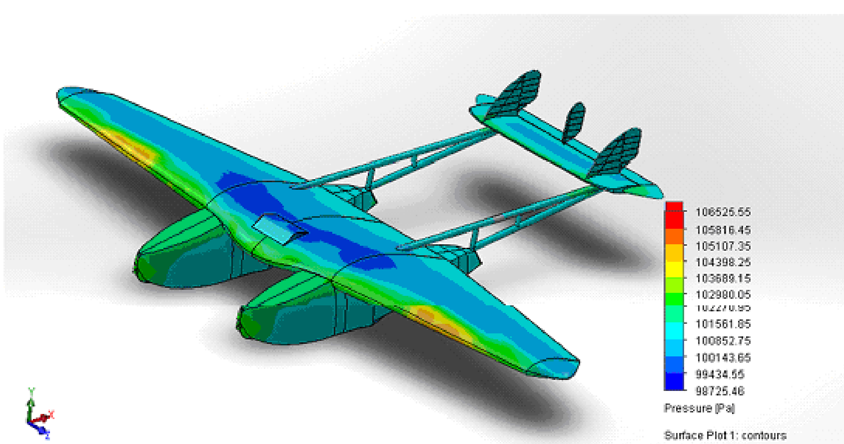

Fig. 7. Pressure distribution over the hydroplane.

3.3 Stress Field

Most stressed parts in the airplane are the wings that support flexural loads*. Scafos* acted as landing gears in modern planes, having however structural function. Wing loading comes mostly from lift obtained in the flow analysis. Primary, secondary and tertiary stresses are present in this part. A plot of equivalent Mises stresses is shown in Fig. 8. As primary and secondary structural members of Jahu were made up of wood, and because of its shape, a quite robust structure resulted, with low stresses. Nonetheless, it was a heavy ship.

Stress analysis used prismatic 3D elements of the library of program SolidWorks, with relative velocity field. Solution procedure included Newton's method. No deformation correction to the loading was applied, as no solid-fluid interaction was pursued. This procedure is deemed unnecessary as the rigidity of the plane, a part its skin, so granted. Boat analyses under take off or sea descending were not considered as well. In this case skin friction with water, mostly, and air, less, would have to be considered with water surface effects.

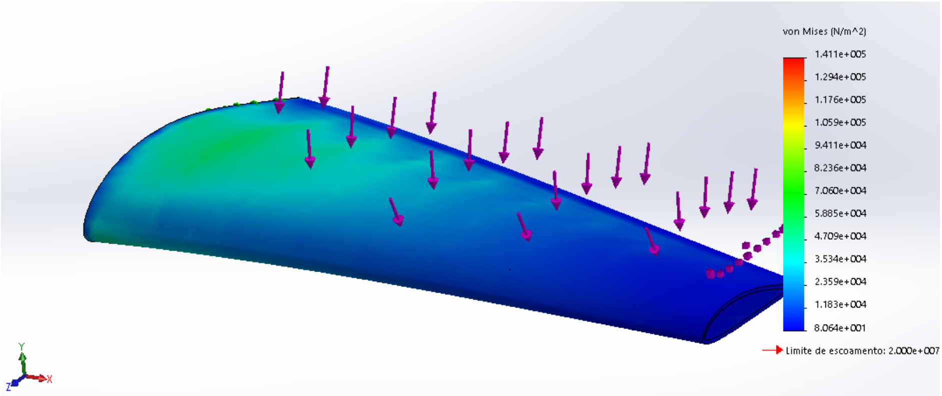

Fig. 8. Stress field in the outer wing model used for structural analysis.

Under level flight, but with stabilizers at 3 degrees, top Mises stresses in the body of the plane were in the range of 50% of the yield stress, with higher values appearing in the boat area, Fig. 9. Wing loads, engines thrusts and efforts transferred to the boats – scafos - by means of the central wing unit are responsible f*or that.* Boats, acting as a double fuselage, also receive loading from the truss system of the tail stabilizers*,* Fig.5.

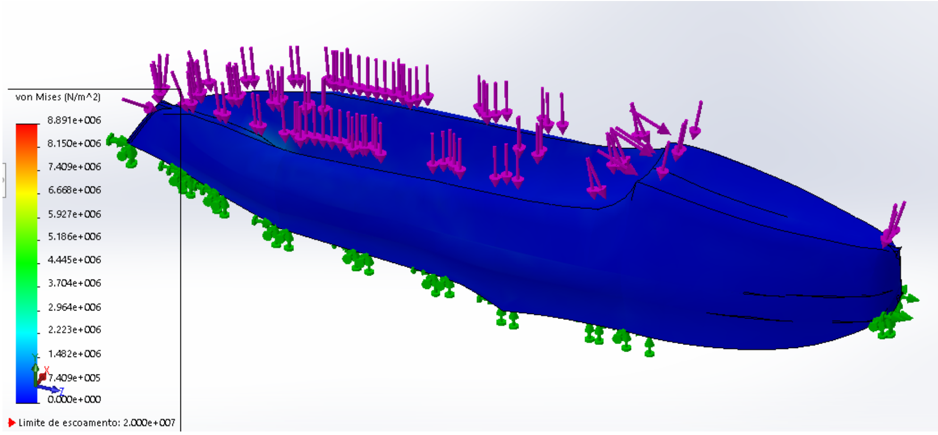

Fig. 9. Air-water loading and Mises stresses in the float unit.

3.4 Discussion

Jahu had an unusual configuration of wings as it had to be positioned inclined during flight. That resulted from its form, size and weight. Table 2 presents obtained results from lift and drag forces.

Variable	Symbol	Value
Drag Force, N	D	23.288 e+03
Lift Force, N	L	42.727 e+03
Drag Coefficient	C_D	0.055
Lift Coefficient	C_L	0.086

Table 2. Flow analysis results.

Values of the drag and lift coefficients, C_D and C_L, defined according to:

$$C_D = \frac{D}{\frac{1}{2}\rho_a A_f v_p{}^2} \tag{30}$$

$$C_L = \frac{L}{\frac{1}{2}\rho_a A_w v^2{}_p} \tag{31}$$

show large values but in the expected range for this type of plane. In the above expressions the areas used are the frontal A_f and projected A_w areas. Tail and main wings were considered. Values obtained for C_D are considered under estimated as the drag component D_E from the pair of engines was not taken into account.

4 I JAHU RELIABILITY

Voyages in the beginning of aeronautics age were characterized by a plague of failures, in part caused by the lack of guidance and control systems, infrastructure, incipient technology and in the case of Jahu, sabotage too. Even though the probability of structural failure of the Jahu was small, because it was a quite robust ship, mechanical failure possibility was appreciable. Here it is an exercise to foresee reliability based on the only flight of Jahu.

The probability of success in each stretch of the journey is based on per hour measures of engine failure probability, at constant speed. Weather conditions, altitude, fuel quality and maintenance, among others, affect this output however. As takeoff, level flight, maneuver and landing phases, have different engine and power rates, an average velocity, the cruse velocity, will be used in each stretch. This avoids integration of probability density functions. Therefore, it is plausible to assume that the probability of success depends on velocity and conditions for each stretch.

Jahu had two engines, working aligned. They were equal, even though they could be working under different conditions. It is assumed here, however, that both had the same service conditions, and obeyed then the same probability function. If the probability of survival of engine 1 after t hours at some cruise, velocity is p_1, and the one for the other, engine 2, is p_2, then necessarily $p_1 = p_2 = p$. As success S, in a stretch of the voyage requires that none of the engines fail, F, completion of the stretch occurs whenever:

$$p_{1\cap 2} = (F_1 \cup S_2) \cap (F_2 \cup S_1) \cap (S_1 \cup S_2) \tag{32}$$

takes place. The probability of failure is 1 - *p*, success p. Therefore:

$$p_{1\cap 2} = p(1-p) + p(1-p) + (1-p)(1-p) = 1 - p^2 \tag{33}$$

Hence the probability of success is p^2. The function $p = \hat{p}(t;C)$ that measures the probability of failure, affected by condition parameter C, is not known explicitly. If a two-parameter Weibull $R = \hat{R}(t;b,\text{q};C)$ reliability function for positive time, in hours, is assumed [9]:

$$R(t) = \exp[-(\frac{t}{\theta})^b]; \quad t \geq 0 \tag{34}$$

then the probability of life *t* of each engine is given by:

$$p(t) = \frac{b}{\theta}(\frac{t}{\theta})^{b-1} R(t) \tag{35}$$

This distribution has an average value μ_t and standard deviation $\hat{\sigma}_t$ determined according to:

$$\mu_t = \theta \Gamma(1 + \frac{1}{b}) \tag{36}$$

$$\hat{\sigma}_t = \theta \sqrt{\Gamma(1+\frac{2}{b}) - \Gamma^2(1+\frac{1}{b})} \quad (37)$$

being Γ the gama function. The cumulative probability function F is determined from the reliability as $F(t) = 1 - R(t)$. In the above, θ corresponds to the life, in hours, for which 63.2 percent of the observations lie below. The skewness parameter is b. Values around 3.3 indicate a symmetric distribution.

For the voyage of the Jahu in the first two stretches, where the engine was working in very adverse conditions, values of θ = 15h and b = 3 were chosen. They correspond to a 13.40 h average life of engines with standard deviation of 4.82 hours. After cleaning the tanks in Gibraltar, it is assumed that conditions improved and values of θ = 20h and b = 3 were, arbitrarily, taken for the next two stretches. Average engine life now was in the order of 18 h with standard deviation of 5 hours. From Praia on, much better performance of the engines were observed, and thus values of θ = 25h and b = 3 were assumed, with engines lasting in average 22.95 hours with deviations around 5.25 hours.

Table 3 lists each of the ten stretches used in the journey of Jahu from Genova, Italy to São Paulo, Brazil. For each step, consumed time was known, or computed from the straight distance between places [10], supposing flight under cruise velocity. The reliability measures the joint probability of success of the whole voyage. It is the conjunction of the fulfillment of the sequence of stretches. If for each step i of the trip, joint probability of success is p_i^2 for the pair of engines, cumulative success probability is $P_i = 1 - R_i$. Supposing independency of the different stretches, joint probability of success is obtained from multiplication of the individual probabilities $\prod_{i=1}^{10} p_i^2$. Therefore, joint reliability computed from sequence in Table 3 gives a value of 0.985615

Stretch i	From/To	Distance d_i km	Time t_i h	Reliability R_i
1	Genova/Alicante	1 070.5	5.00	0.999847
2	Alicante/Gibraltar	495.6	2.98	0.999999
3	Gibraltar/Gran Canary	1 324.	7.25	0.999960
4	Gran Canary/Praia	1 646.	9.43	0.999457
5	Praia/Fernando de Noronha	2 307.	12.144	0.986947
6	Fernando de Noronha/Natal	375.	2.26	0.999999
7	Natal/Recife	254.5	1.53	0.999999
8	Recife/Salvador	672.6	4.05	0.999998
9	Salvador/Rio de Janeiro	1 209.2	7.28	0.999390
10	Rio de Janeiro/São Paulo	360.7	2.17	0.999999

Table 3. Success estimates of Jahu´s voyage per step.

Evidently the voyage couldn´t be completed in one stretch only, not even two. With three stretches, first one starting in Genova and ending in Praia, consuming a time of 24.66

hours, second from Praia to Fernando de Noronha, consuming the 12.144 hours realized, and finally the Brazilian coast stretch taking 17.28 hours was a possible journey with engines in good conditions. Reliability for this sequence would be of 0.896.

5 | CONCLUSIONS

Progetto S55 was under way in Italy by 2016 to construct and fly a replica of Savoia-Marchetti S-55 to South America [11]. This was in part due to the importance of Savoia-Marchetti to the history of aeronautics in Italy. Jahu, besides making part of that history, is one of the last of such planes still in good conditions. In the museum of TAM in São Carlos, Brazil, the complete airplane, after a restoration undertaken in São Paulo, is exposed. This work addresses the understanding of the design of such an important aircraft to the development of airplane industry.

It is seen that the airplane had some different concepts. Its aerodynamics shows large values of drag and lift coefficients that deemed the plane very consuming. Fact confirmed by the crew decision of dropping most of the equipment that came with it, in order to save space for the tanks of fuel. Lift obtained for zero angle of attack was smaller than the weight of the plane, what required “using wing at level flight”. Structural arrangement of wings and its analysis confirms that structurally speaking, Jahu was a sound plane. Repositioning structural components in the original arrangement, however, could make it easier to fly.

Additional work is necessary to finish the structural analysis of the plane, incomplete at this point, as different flight situations weren´t analyzed, neither the dynamic response produced. But so far it confirms the robustness of the plane. Investigations on alternative woods, if kept that option, for construction of a lighter replica are important as they lead to less power, even keeping the form of the plane. A hydroplane for conditions in Amazonia, well in demand nowadays, could also use results from the present study.

ACKNOWLEDGMENTS

Making available some drawings used in the development of the model by Progetto S55 [12] is dully acknowledged.

REFERENCES

[1] https://pt.wikipedia.org/wiki/Jahu_(hidroavião)

[2] Idrovolante “Savoia Marchetti” tipo S. 55 X, Istbuzioni per il montaggio e per la regolaziche.

[3] Gurtin, E., *Continuum Mechanics*, John Wiley, 2002

[4] Stengel, Robert F., *Flight Dynamics*, Princeton University Press. Princeton, 2004, ISBN 0-691-11407-2.

[5] Zienkiewicz, O, Taylor, R. and Zhu, J.Z. ¨The Finite Element Method: Its Basis and Fundamentals¨, 7th edition, 2003, Elsevier

[6] Belytschko, T. and Fish, J., *A First Course in Finite Elements*, John Wiley, 2010

[7] Bathe, K. J., *Finite Element Procedures in Engineering Analysis*, Prentice-Hall, 2nd Edition, 1996

[8] SolidWorks, Student's Guide to Learning, Dassault Systemes, 2013

[9] Budynas. R.G. and Nisbett, J.K., *Shigley´s Mechanical Engineering Design*, 8th edition, SI Units, McGraw-Hill Companies, Inc., NY, USA, 2008

[10] https://www.distancefromto.net

[11] https://www.progetto55.it/chi-siamo

[12] Progetto S55, Study Program 55, Busto Arsizio (Va), Italy, 201

ÍNDICE REMISSIVO

P

R

S

T

U

V

W

COLEÇÃO

DESAFIOS DAS ENGENHARIAS:

ENGENHARIA DE COMPUTAÇÃO 2

www.atenaeditora.com.br

contato@atenaeditora.com.br

@atenaeditora

www.facebook.com/atenaeditora.com.br

Atena Editora

Ano 2021

COLEÇÃO

DESAFIOS DAS ENGENHARIAS:

ENGENHARIA DE COMPUTAÇÃO 2

www.atenaeditora.com.br
contato@atenaeditora.com.br
@atenaeditora
www.facebook.com/atenaeditora.com.br

Atena Editora
Ano 2021